


RESEARCH PAPER

 OPEN ACCESS 

miR-148b-3p, as a tumor suppressor, targets son of sevenless homolog 1 to regulate the malignant progression in human osteosarcoma

Guodong Liu, Honggang Mao, Yan Liu, Zun Zhang, Si Ha, and Xiaoyan Zhang 

Department of Orthopedics, Baogang Hospital (The Third Affiliated Hospital of Inner Mongolia Medical University), Baotou, Inner Mongolia, People's Republic of China

ABSTRACT

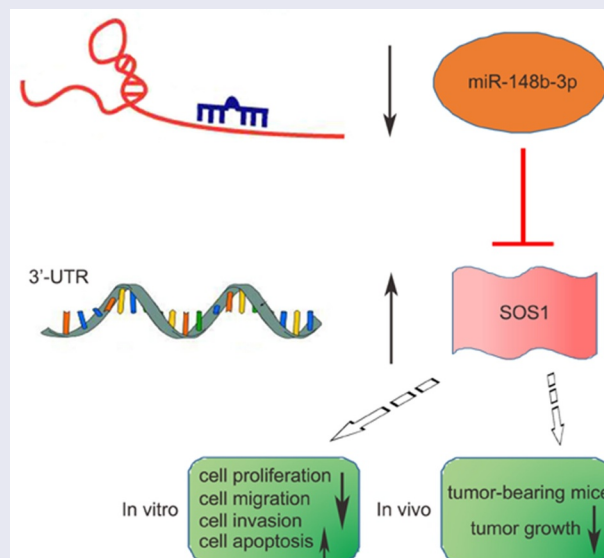
Osteosarcoma (OS) is a malignant tumor that occurs in children and adolescents. Previous studies reported a low expression of miR-148b-3p in OS, but its biological function in OS remains obscure. This study aimed to explore the role of miR-148b-3p in OS progression. Herein, the expression of miR-148b-3p and son of sevenless homolog 1 (SOS1) both in OS tissues and cells were examined using quantitative real-time polymerase chain reaction and Western blotting assay. miR-148b-3p mimic or inhibitor, pcDH-SOS1 plasmid or si-SOS1 and agomir-miR-148b-3p were constructed for cell transfection. *In vitro*, the biological effect of miR-148b-3p was determined employing MTT, EdU, colony formation, flow cytometry, transwell and wound healing assay, separately. The target relationship between SOS1 3'-untranslated region (3'-UTR) and miR-148b-3p was analyzed using dual-luciferase reporter gene. *In vivo*, the inhibition of agomir-miR-148b-3p in mice was evaluated via a xenograft mouse model. miR-148b-3p was noticeably low-expressed in OS tissues and cells, and miR-148b-3p over-expression in OS cells suppressed the growth, migration and invasion, induced apoptosis. The effect of miR-148b-3p-inhibitor on cell biological behavior is opposite to that of miR-148b-3p over-expression. Conversely, The expression of SOS1 was significant higher in OS tissues and cells, miR-148b-3p targeted and was negatively associated with the expression level of SOS1. In addition, the anti-tumor effect of miR-148b-3p was reversed by SOS1. Importantly, we demonstrated that the tumor growth of stably over-expressed miR-148b-3p human MG-63 cells was obviously reduced in tumor-bearing mice. These data highlighted that miR-148b-3p might be as a promising therapeutic target for OS.



ARTICLE HISTORY

Received 28 September 2021
Revised 9 January 2022
Accepted 12 January 2022

KEYWORDS

miR-148b-3p; SOS1; osteosarcoma; tumor suppressor



CONTACT Xiaoyan Zhang  zhangxyimar@aliyun.com  Department of Orthopedics, Baogang Hospital (The Third Affiliated Hospital of Inner Mongolia Medical University), No. 20, Shaoxian Road, Baotou, Inner Mongolia, 014010, People's Republic of China

© 2022 The Author(s). Published by Informa UK Limited, trading as Taylor & Francis Group.

This is an Open Access article distributed under the terms of the Creative Commons Attribution-NonCommercial License (<http://creativecommons.org/licenses/by-nc/4.0/>), which permits unrestricted non-commercial use, distribution, and reproduction in any medium, provided the original work is properly cited.

Introduction

Osteosarcoma (OS) is a primary pernicious bone tumor that severely threatens the lives and healths of children and adolescents, and often occurs in the first or second decade [1,2]. OS originates from malignant mesenchymal cells [3], which can disrupt bone formation and osteoblast/osteoclast activity balance [4], resulting in pathological fractures and bone metastases. Advanced OS has a high degree of malignancy, poor prognosis, accompanied by local recurrence and lung metastasis [5]. At present, the best clinical treatment is tumor resection combined with adjuvant chemotherapy, which greatly improves the prognosis of OS patients, and its 5-year survival rate is about 65–70% [6]. Unfortunately, once the patient has metastasis or recurrence, only 10–20% of patients survived over 5 years [7].

MicroRNA (miRNA), a kind of small non-coding single-stranded RNA (ncRNA) containing about 19–23 nucleotides, act a considerable role in endogenous gene regulation through mediating translational repression or promoting the degradation of the target mRNA [8]. In recent decades, miRNAs have drawn increasing attention from scientists, especially for their role in a variety of cancers and other diseases [9]. Studies have found that miRNAs can target more than 30% of the human genome, and abnormal expression of which is closely connected with the occurrence of various cancers [10]. miR-148-3p, as a novel miRNA, has abnormal levels in many types of cancers. Zhang et al. reported that miR-148b-3p expression was downregulated in renal cancer and involved in FGF2-FGFR2 signal transduction [11]. Li et al. found miR-148-3p was downregulated and reduced the motility of gastric cancer cells through targeting Dock6 [12]. Also, studies have shown that miR-148b-3p was significantly downregulated and reduced miR-148b-3p is negatively relevance with poor overall survival of gastrointestinal stromal tumors [13]. According to our best knowledge, the regulatory role of miR-148-3p in OS has rarely been reported. Liu et al. first found that miR-148-3p was low-expressed in stage I and II paraosseous OS tissues and was related to a poor clinical prognosis [14]. However, the clear mechanism of miR-148-3p on OS progression has not been elucidated.

Son of sevenless homolog 1 (SOS1), a member of the SOS family, is a cohesion protein that plays an important role in the intracellular signal transduction pathways [15]. Abnormal expression or mutation of SOS1 was found to be associated with a clinical disease [16]. Chen et al. found that SOS1 was dysregulated in ovarian cancer and promoted its metastasis [17]. Whether SOS1 deregulation mediates the biological behavior of OS is unclear. miRNAs bind to 3' – UTRs (3' – untranslated regions) of downstream target to inhibit their transcriptional and post-transcriptional regulation [18]. Therefore, we tried to further verify the role of miR-148-3p in OS *in vitro* and *in vivo*.

In this study, bioinformatics screening indicated that SOS1 might be a potential target gene of miR-148-3p. We hypothesized the miR-148-3p/SOS1 axis plays a role in OS progression. We performed a series of functional experiments to explore the regulatory mechanism during OS malignancy to support this assumption. This paper reported for the first time that miR-148b-3p could antagonize the malignant behavior of human OS cells, and enriched our understanding of miR-148-3p involvement in OS progression.

Methods and materials

Source of tissue samples

This study was authorized by the ethics committee of Inner Mongolia Medical University and strictly implemented the Declaration of Helsinki formulated by the World Medical Association (WMA). This study obtained the consent of all donors and signed informed consent. A total of 41 first diagnosed and treated patients between April 2016 and February 2019 with OS (mean age 12.16 ± 13.18 years, range 8 to 39 years) without other malignancies and systemic disease, and adjacent normal soft tissue from the same donor were included. Immediately after resection, the OS tissues and normal soft tissues were placed liquid nitrogen and transferred to -80°C for subsequent experiments.

Cell culture

Human OS cell lines (MG-63, U2OS) and osteoblast cell line (hFOB 1.19) were obtained from

ATCC (Manassas, VA, USA). The cells were cultivated in Dulbecco's modified Eagle's medium (DMEM) or RPMI-1640 (Gibco, Grand Island, NY, USA) with 10% FBS (HyClone, Logan, UT, USA) and Penicillin-Streptomycin Liquid (Solarbio, Beijing, China) in a humidified constant temperature incubator at 37°C, 5% CO₂.

RNA transfection *in vitro*

miR-148b-3p negative control (miR-NC) and mimic, miR-148b-3p negative control (NC-inhibitor) and miR-148b-3p-inhibitor were obtained from GenePharma (Shanghai, China). Briefly, according to the manufacturer's protocols, OS cells (MG-63 and U2OS) at 5×10^5 cells/well in a 12-well plate were transfected with 1 µg of mimics or miR-NC, miR-148b-3p-inhibitor or NC-inhibitor by Lipofectamine 3000TM (Invitrogen Life, Carlsbad, CA, USA). Otherwise, miR-148b-3p mimics or miR-148b-3p-inhibitor were co-transfected with 4 µg pcDH-SOS1 plasmid or si-SOS1 (GeneChem, Shanghai, China) per well. Cell transfection efficiency was measured after 48 h [12].

Quantitative real-time polymerase chain reaction (qRT-PCR) assay

According to the manufacturer's protocols, the mRNA of OS tissues and cells were isolated using the TRIzol RNA isolation kit (Invitrogen Life, Carlsbad, CA, USA), respectively. The cDNA of tissues and cells were synthesized by a cDNA Synthesis Kit (Takara Bio, Shiga, Japan), followed by kept at -20°C. The qRT-PCR assay was performed applying SYBR Premix Ex Taq (Takara Bio, Shiga, Japan). The $2^{-\Delta\Delta C_t}$ method was calculated the relative quantitative values of genes [19]. GAPDH or U6 was used as an internal control. The primer sequences used in this study were as follows:

miR-148b-3p Forward (F): 5'-GCGTCAG TGCATCACAGAACTTTGT-3', Reverse (R): 5'-CGAATTCTAGAGCTCGAGGCAGGCGACA-3'; U6 F: 5'-GCTTCGGCAGCACATATACTAAAAT-3', R: 5'-CGCTTCACGAATTTGCGTGCAT-3'; SOS1 F: 5'-CGTGAATTCGCTGCAACA TGGTGGAAC-3', R: 5'-TCACTCGAGGT GGGCTATGTAAGGCATTTTTC-3'; GAPDH' F

5'-AACGGATTTGGTCGTATTG-3', R: 3'-GGAAGATGGTGATGGGATT-3'.

MTT assay

MG-63 and U2OS cells pretreated with mimic or miR-148b-3p-inhibitor were inoculated into a 96-well culture plate (Corning, NY, USA) about a density of 5×10^3 cells/well, with six replicates per group. 20 µl of 5 mg/mL MTT solution (Sigma-Aldrich, Waltham, MA, USA) was supplemented into each well at 0, 24, 48 or 72 h post cell inoculation, and continued for 4 h. Cell suspension was cleared, 200 µl DMSO (Sigma-Aldrich, Waltham, MA, USA) was supplemented into every well, and incubated for another 10 min [11]. The absorbance at 490 nm was detected by a Bio-Rad xMark microplate reader (Bio-Rad, California, USA). The steps were replicated in triplicate.

5-Ethynyl-2'-deoxyuridine (EdU) staining

EdU labeling assay was used to text the cell proliferation by EdU Staining Proliferation Kit (iFluor 647, Abcam, Cambridge, UK). OS cells were seeded into a 6-well plate (1×10^4 cells/well) and routinely incubated for 24 h [20]. A total of 50 µM EdU solution was added well for 2 h under dark conditions, according to the manufacturer's protocols. The cells were incubate with fixative solution at 37°C for 15 min, and added reaction mix to fluorescently label EdU and incubated for 30 min. Finally, visualized images were analyze by a fluorescence microscope (Olympus, Tokyo, Japan).

Colony formation assay

First of all, the basal agar glue supplemented with 1.2% agarose was prepared in 6-well plates (Corning, NY, USA). 24 h after transfection, MG-63 and U2OS cells (1.5×10^3 cells/well) mingled with 1 ml complete medium containing 0.7% agarose (Sigma-Aldrich, Waltham, MA, USA) were seeded into above 6-well plates for 2 consecutive weeks [15]. After that, 5 ml of 4% paraformaldehyde was added to fix cells for 15 min, then the fixative was removed, and appropriate Gimsa was added to stain cells for 20 min

(Solarbio, Beijing, China). The numbers of cell colonies were counted by an optical microscope (Nikon, Tokyo Metropolis, Japan). The steps were replicated in triplicate.

Wound healing assay

24 h after transfection, single-cell suspension was prepared with 10% FBS (HyClone, Logan, UT, USA). 5×10^5 cells were seeded into each well of 6-well culture plates (Corning, NY, USA), which covered at the bottom of 6-well plates [21]. When the cells reached 90% confluence, each well was straightly scratched 3 times with a properly sized sterile pipette tip. After rinsing with PBS for 3 times, the cells were maintained in serum-free medium (Gibco, Grand Island, NY, USA). The photographs of wound closure at 0 h or 24 h were captured under a light microscope (Nikon, Tokyo Metropolis, Japan). Relative mobility = migration area of miR-148b-3p group/migration area of miR-NC group.

Transwell assay

The invasive ability of OS cells was examined with transwell chamber (Corning, NY, USA). 24 h after transfection, about 5×10^5 cells resuspended in 200 μ l serum-free medium (HyClone, Logan, UT, USA) were inoculated into the upper chambers covered with Matrigel (BD, San Jose, CA, USA). A further 600 μ l of culture medium with 5 μ g/ml fibronectin (BD, San Jose, CA, USA) was added to the lower chamber. Post 24 h incubation, the non-invasive cells were swabbed with a sterile swab and rinsed with PBS [15]. The invasive cells were immobilized with 95% ethanol, and then stained using 0.1% crystal violet (Sigma-Aldrich, Waltham, MA, USA). A light microscope (Nikon, Tokyo Metropolis, Japan) was used to randomly acquire five visible areas for imaging and counting. The steps were replicated in triplicate.

Apoptosis analysis

MG-63 and U2OS cell lines were inoculated into 6-well plates (Corning, NY, USA) with 5.0×10^5 cells/well, followed by transfection with mimic or miR-148b-3p-inhibitor for 48 h [15]. Then, they

were harvested and cleaned twice with PBS. Cells were stained with an Annexin V-FITC/PI fluorescence double-staining kit (Solarbio, Beijing, China) for 15 min, according to the manufacturer's protocols. The distribution of fluorescence scatter was analyzed by a flow cytometer (BD, NJ, USA). The steps were replicated in triplicate.

Luciferase report analysis

We used TargetScan (<http://www.targetscan.org/>) online tool to predict downstream target genes of miR-148b-3p. Wild type SOS1 (SOS1-WT) and mutant SOS1 (SOS1-MUT) plasmid vectors were constructed from GenePharma (Shanghai, China). Then, SOS1-WT or SOS1-MUT was co-transfected with mimic/miR-NC into MG-63 and U2OS cells by Lipofectamine™ 3000 Transfection Reagent (Invitrogen, Waltham, USA), respectively [12]. 48 h later, the luciferase activity was examined employing a Dual-Luciferase® Reporter (DLR™) Assay System (Promega, Springfield, USA).

Western blotting (WB) analysis

The total protein samples from OS cells and tumor-bearing mice tissues were treated with RIPA lysis buffer (Sigma-Aldrich, Waltham, MA, USA). Then, above extraction content was quantitatively analyzed using a BCA kit (Beyotime, Haimen, China). Next, protein samples were distributed by 12% SDS-PAGE (Beyotime, Haimen, China) and transferred onto a PVDF membrane (Millipore, Billerica, MA, USA). The PVDF membranes containing target proteins were sealed for 2 h with 5% defat milk at room temperature. Subsequently, the specific primary antibodies were incubated at 4°C overnight [12]. The antibodies were listed as followed: SOS1 (#5890, CST, Massachusetts, USA), β -actin (#4970, CST, Massachusetts, USA). The next day, horseradish peroxidase (HRP)-labeled secondary antibody (Beyotime, Haimen, China) were utilized to couple with indicated SOS1 antibody. Finally, the films were visualized using a BeyoECL Moon kit (Beyotime, Haimen, China).

Xenograft model *in vivo*

All animal models in this study complied with the Guide to Care and Use of Laboratory Animals and were authorized by the ethical committees of Inner Mongolia Medical University. 4 weeks old female BALB/c nude mice (12 ± 2 g) without specific pathogens (SPF) were obtained from Vital River Laboratories (Beijing, China), who were placed in an appropriate environment to get clean water and food. Referring to the previous methods [21], about 5×10^6 MG-63 cells were injected under the lateral proximal of left tibia of the BALB/c nude mice. They were separated into 2 groups ($n = 6$): agomir-NC and agomir-miR-148b-3p group. When the volume of tumor reached 100 mm^3 , $100 \mu\text{l}$ agomir-miR-148b-3p or agomir-NC was intratumourly injected every 3 days. The maximum diameter (expressed as a) and minimum diameter (expressed as b) of the xenograft tumors were detected per day, and the volume ($V = ab^2/2$) was counted. 35 days later, all animals were sacrificed, and tumor tissues were harvested for further analysis.

Immunohistochemistry (IHC)

The tumors of transplanted mice were fixed with 4% paraformaldehyde, followed by embedding in paraffin. Before the experiment, $4 \mu\text{m}$ slices were dewaxed and rehydrated. Secondly, the samples were sealed with 3% hydrogen peroxide for 10 min at room temperature, and the primary antibody against PCNA, MMP9 and cleaved-caspase-3 were incubated at 4°C overnight after antigen repair. The indicated secondary antibody was incubated at 25°C for 30 min [21]. Finally, the sections were re-stained with hematoxylin for 2 min, and dehydrated and sealed for analysis.

Statistics analysis

All data were illustrated as mean \pm SEM and analyzed by SPSS 23.0 (IBM, Armonk, USA). All independent experiments were repeated at least three times. Differences analysis were evaluated using two-tailed Student's *t*-test or one-way ANOVA followed by Dunnett's post hoc test. *P* value <0.05 in any analysis was regarded as a statistically significant difference.

Results

We aimed to validate the anti-tumor effect of miR-148b-3p in OS *in vitro* and *in vivo*, and further investigate the regulatory association between miR-148b-3p and SOS1 as well as their roles in OS progression.

Abnormal expression of miR-148b-3p and SOS1 in OS tissues and cell lines

Substantial evidences suggest that miRNA plays an important regulatory role in tumor progression. miR-148b-3p, which had rarely been studied in OS, was selected for this study. qRT-PCR analysis revealed the mRNA level of miR-148b-3p was lower in OS tissues than para-carcinoma tissues (Figure 1a), and the mRNA level of SOS1 was higher in OS tissues than para-carcinoma tissues (Figure 1b). In addition, correlation coefficient analysis indicated SOS1 expression were negatively associated with miR-148b-3p in OS tissues (Figure 1c). Also, we discovered that the protein expression of SOS1 in OS tissues was elevated (Figure 1d). Furthermore, we examined the mRNA level of miR-148b-3p and SOS1 in OS cells. Compared with osteoblasts hFOB1.19 cell, the mRNA level of miR-148b-3p was down-regulated in MG63 and U2OS cell lines (Figure 1e). Consistently, SOS1 was also highly expressed in MG63 and U2OS cell lines (Figure 1f and g).

miR-148b-3p over-expression restrained OS cell proliferation

In order to evaluate the functional role of miR-148b-3p in OS cells, miR-148b-3p mimic and miR-NC were transfected into MG-63 and U2OS cell lines, respectively, and their transfection efficiency detected by qRT-PCR analysis. Compared with miR-NC group, we found a significant increase in miR-148b-3p mRNA levels (Figure 2a). Moreover, we also evaluated the proliferation rate of OS cells using MTT (Figure 2b and c), EdU staining (Figure 2d and e) and colony formation (Figure 2f and g) experiments. The results showed the proliferation abilities of MG-63 and U2OS cells were significantly decreased post transfection with mimics.

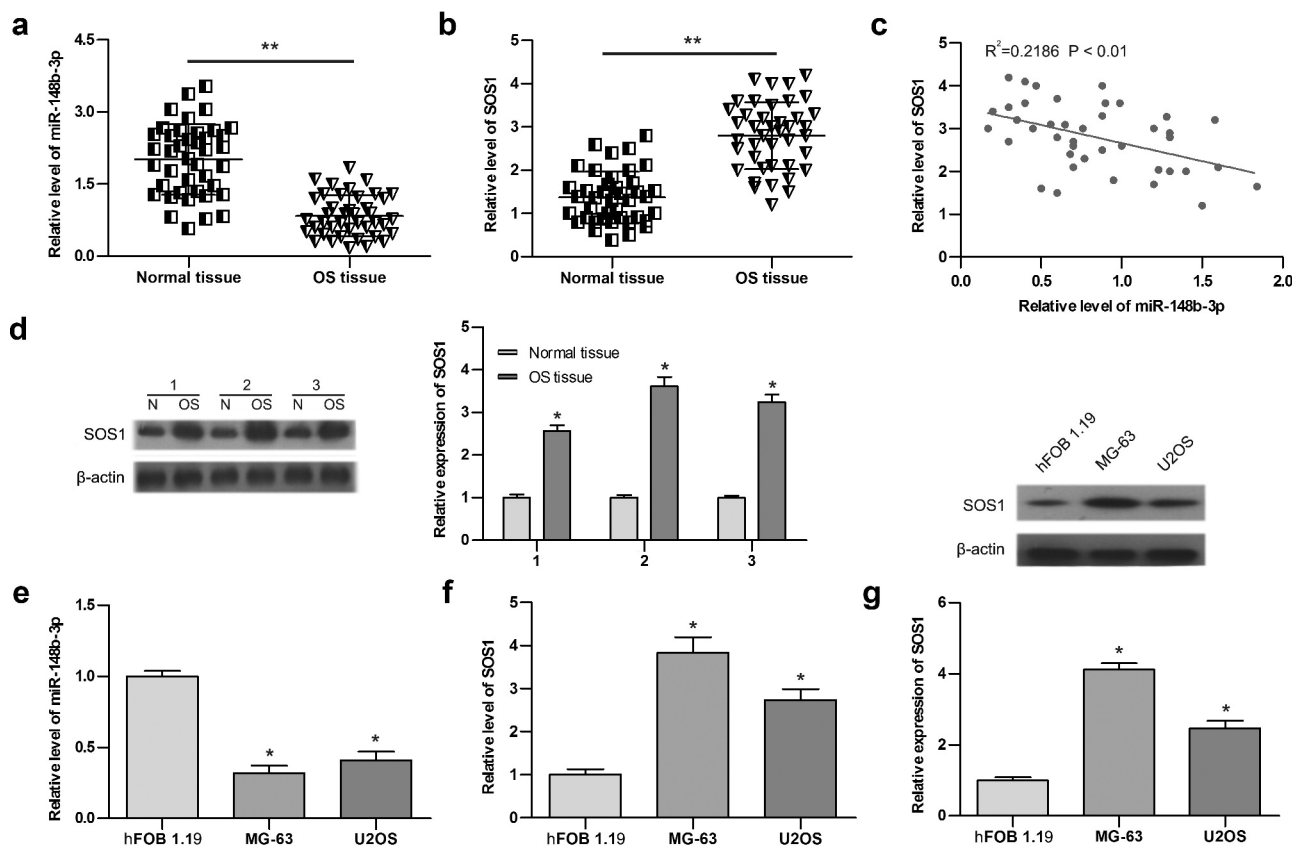


Figure 1. miR-148b-3p was lowly expressed in OS tissues and cells. (a) The mRNA level of miR-148b-3p in tumor and para-carcinoma normal tissues was analyzed using qRT-PCR. (b) The mRNA level of SOS1 in tumor and para-carcinoma normal tissues was analyzed using qRT-PCR. (c) The correlation analysis between miR-148b-3p and SOS1. (d) The protein expression of SOS1 in tumor and para-carcinoma normal tissues was analyzed using WB assay. (e) The mRNA level of miR-148b-3p in osteoblast and OS cells was determined using qRT-PCR. (f) The mRNA level of SOS1 in osteoblast and OS cells was determined using qRT-PCR. (g) The protein expression of SOS1 in osteoblast and OS cells was analyzed using WB assay. * $P < 0.05$, ** $P < 0.01$ versus normal tissues or normal osteoblast cells.

miR-148b-3p over-expression restrained the migration and invasion, and induced apoptosis in OS cells

Subsequently, the effect of miR-148b-3p on the migratory ability of OS cells (MG-63 and U2OS) were detected using wound-healing test. Compared with the miR-NC group, miR-148b-3p mimic significantly reduced the wound closure rate of OS cells (Figure 3a). Similarly, miR-148b-3p mimic obviously decreased the invasive ability of OS cells compared with the miR-NC (Figure 3b). As shown in Figure 3c, the apoptotic percentage of cells was apparent higher in over-expressed miR-148b-3p group than in miR-NC group. These data indicated that over-expressed miR-148b-3p suppressed the migratory and invasive abilities, and induced apoptosis of OS cells.

miR-148b-3p inhibition promoted OS cell proliferation

To explore the effect of miR-148b-3p inhibition in OS cells, miR-148b-3p-inhibitor and NC-inhibitor were transfected into MG-63 and U2OS cell lines, respectively, and their transfection efficiency detected by qRT-PCR analysis. There was a significant decrease of miR-148b-3p mRNA level in miR-148b-3p-inhibitor group (Figure 4a). Furthermore, the proliferation rate of OS cells were evaluated using MTT (Figure 4b and c), EdU staining (Figure 4d and e) and colony formation (Figure 4f and g) experiments. The above results indicated the proliferation abilities of OS cells were significantly increased post transfection with miR-148b-3p-inhibitor.

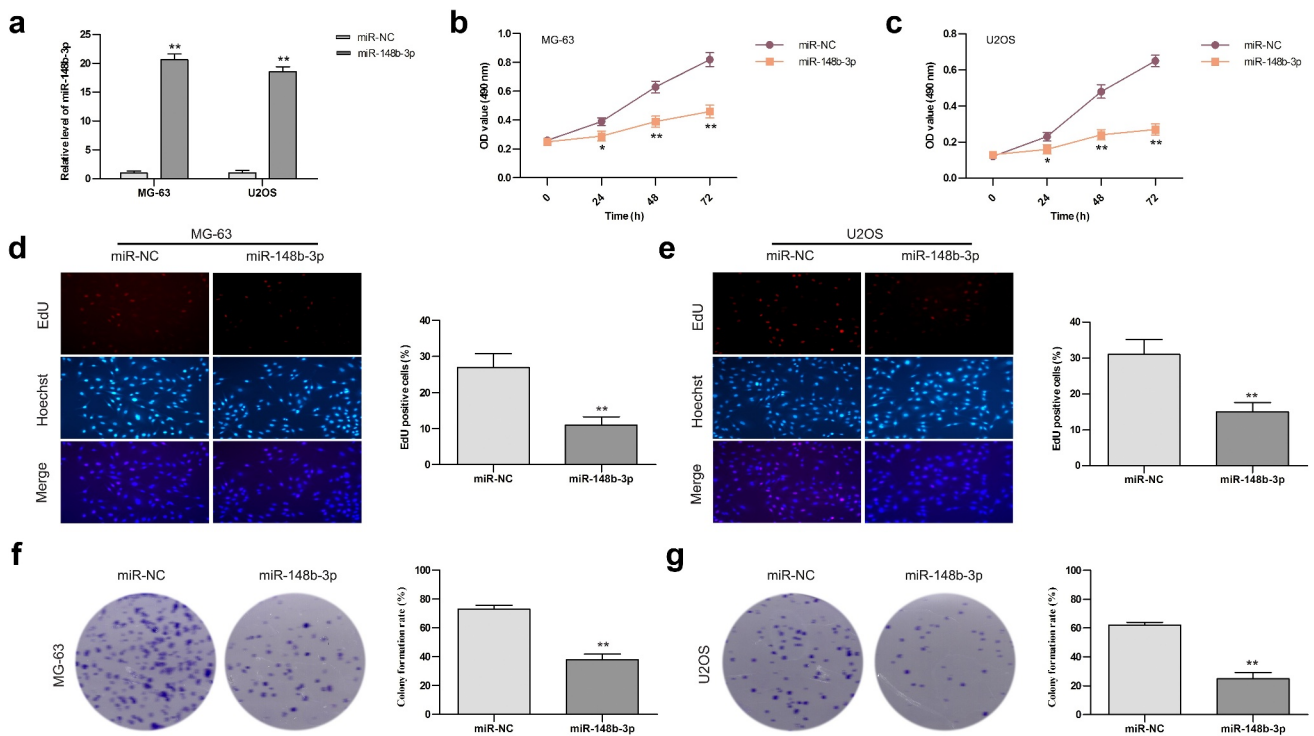


Figure 2. The effects of miR-148b-3p overexpression on the growth of MG-63 and U2OS cells. (a) The mRNA level of miR-148b-3p was detected in MG-63 and U2OS cells post transfection with mimics. (b) The viability of MG-63 cells was tested using MTT assay. (c) The viability of U2OS cells was tested using MTT assay. (d) MG-63 cells proliferation was determined by EdU assay. (e) U2OS cells proliferation was determined by EdU assay. (f) The colony number of MG-63 cell was counted by colony formation assay. (g) The colony number of U2OS cell was counted by colony formation assay. *P < 0.05, **P < 0.01 versus miR-NC.

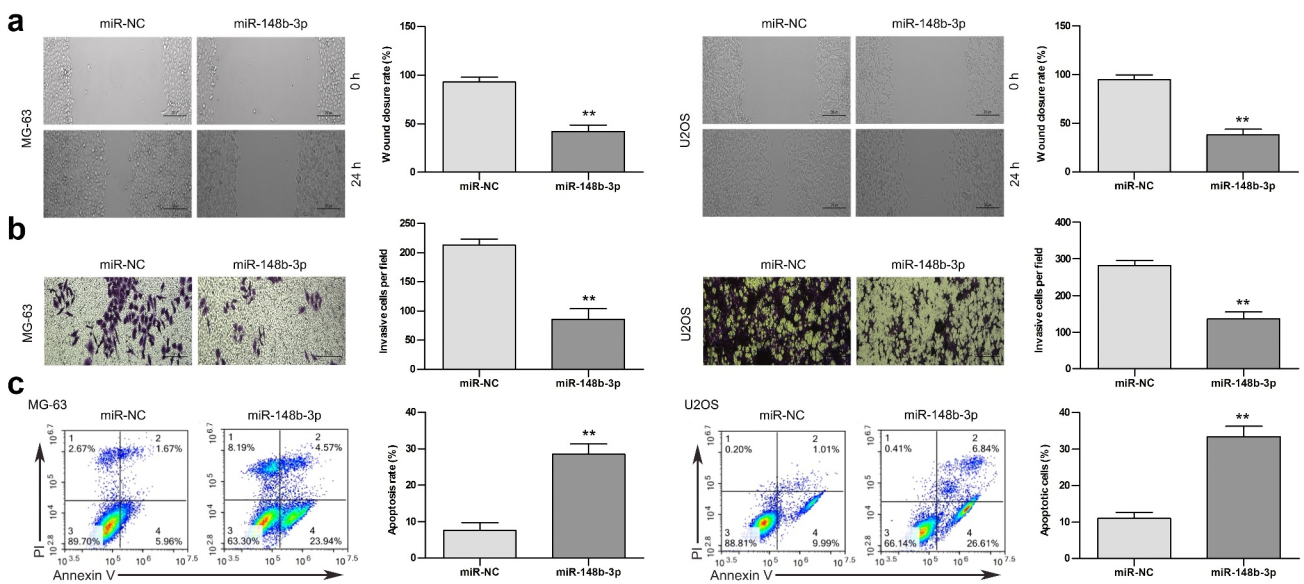


Figure 3. The effects of miR-148b-3p overexpression on the migration, invasion and apoptosis of MG-63 and U2OS cells. (a) The migratory ability of OS cells were measured using wound healing test, scale bars = 200 μ m. (b) The invasive ability of OS cells were using transwell invasion assay, scale bars = 200 μ m. (c) The apoptotic rate of OS cells was checked by flow cytometry. **P < 0.01 versus miR-NC.

miR-148b-3p inhibition promoted the migration and invasion, and suppressed apoptosis in OS cells

After transfection of miR-148b-3p inhibitor and NC-inhibitor in OS cells, we further detected the anti-tumor effect of miR-148b-3p. Compared with the NC-inhibitor group, miR-148b-3p inhibitor obviously increased the wound closure rate (Figure 5a), significantly enhanced the invasive ability of OS cells (Figure 5b). The apoptotic percentage of cells was clear lower in miR-148b-3p inhibitor group than in NC-inhibitor group (Figure 5c). These data indicated that miR-148b-3p inhibition accelerated the migratory and invasive abilities, and restrained apoptosis of OS cells.

miR-148b-3p directly bound to SOS1 in OS cells

The above results indicated that miR-148b-3p could be used as a tumor suppressor, and

SOS1 expression were negatively associated with miR-148b-3p. According to TargetScan online, SOS1 was predicted to be a potential target gene of miR-148b-3p, Figure 6a showed that SOS1 3' -UTR might be a functional target site of miR-148b-3p. Then, we stably transfected miR-148b-3p mimics or miR-NC into both MG-63 and U2OS cells for 24 h. Compared with miR-NC, the luciferase activity of the wild-type 3' -UTR-SOS1 (SOS1 WT) dramatically decreased, while mutant 3' -UTR-SOS1 (SOS1 MUT) showed little change (Figure 6b and c). In addition, we found a significant decrease of SOS1 expression in OS cells post miR-148b-3p mimic transfection, But this alteration was reversed by SOS1 overexpression (Figure 6d and e). Accordingly, the change of SOS1 protein level was consistent with the mRNA level (Figure 6f). The above results demonstrated that SOS1 was the target gene of miR-148b-3p, and over-expressed miR-148b-3p decreased the expression of SOS1.

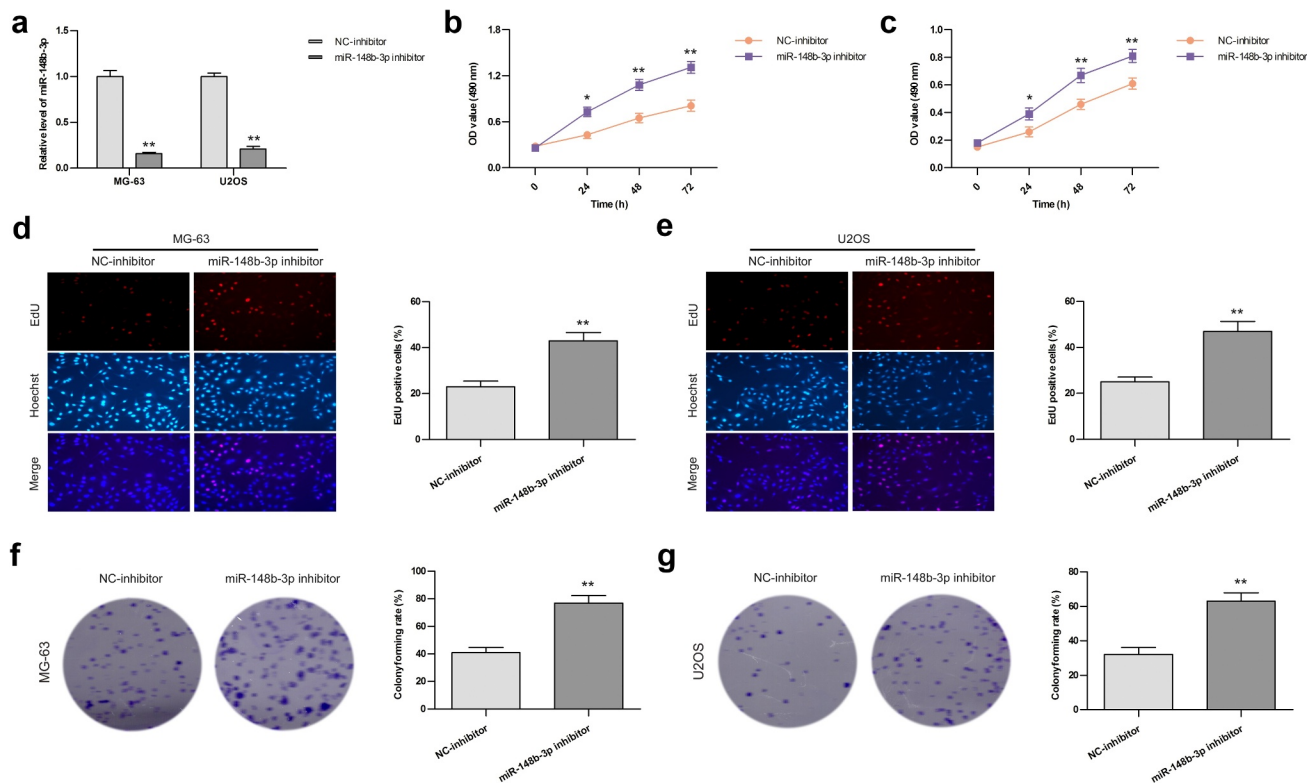


Figure 4. The effects of miR-148b-3p inhibition on the growth of MG-63 and U2OS cells. (a) The mRNA level of miR-148b-3p was detected in MG-63 and U2OS cells post transfection with miR-148b-3p inhibitor. (b) The viability of MG-63 cells was tested using MTT assay. (c) The viability of U2OS cells was tested using MTT assay. (d) MG-63 cells proliferation was determined by EdU assay. (e) U2OS cells proliferation was determined by EdU assay. (f) The colony number of MG-63 cell was counted by colony formation assay. (g) The colony number of U2OS cell was counted by colony formation assay. *P < 0.05, **P < 0.01 versus NC-inhibitor.

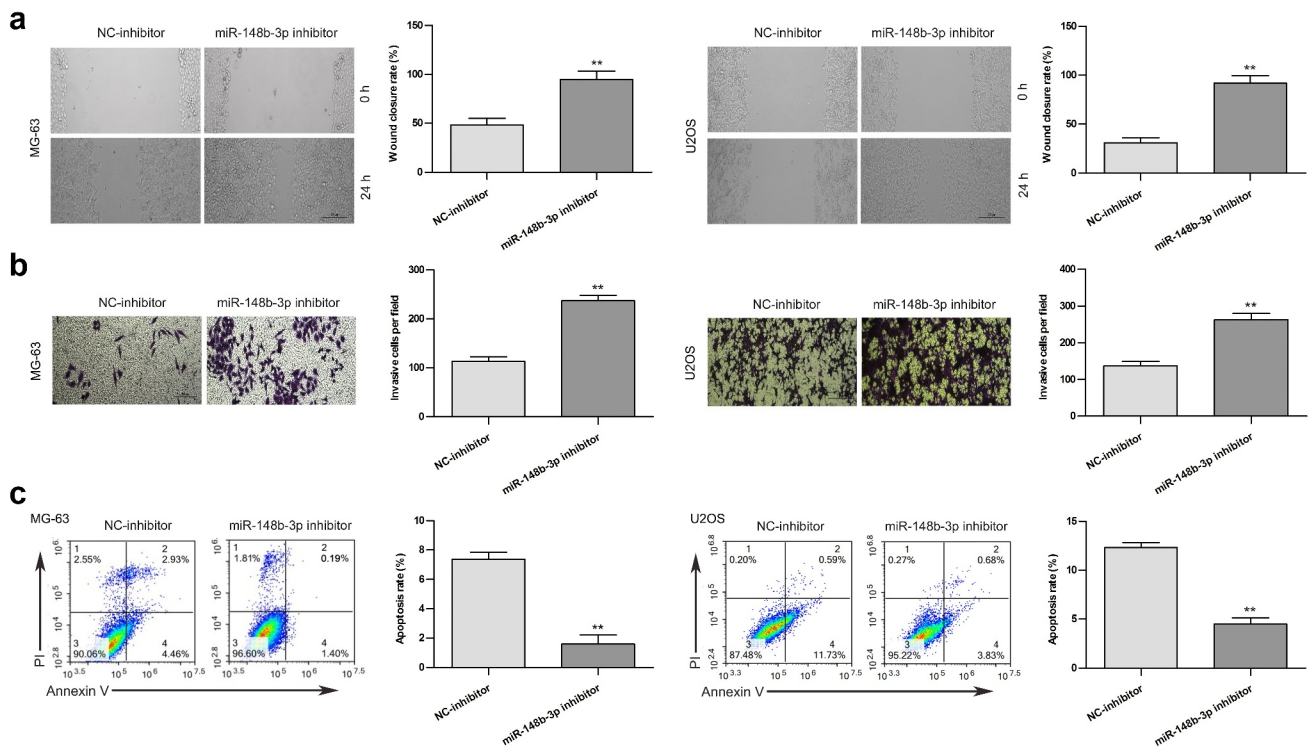


Figure 5. The effects of miR-148b-3p inhibition on the migration, invasion and apoptosis of MG-63 and U2OS cells. (a) The migratory ability of OS cells were measured using wound healing test, scale bars = 200 μ m. (b) The invasive ability of OS cells were using transwell invasion assay, scale bars = 200 μ m. (c) The apoptotic rate of OS cells was checked by flow cytometry. **P < 0.01 versus NC-inhibitor.

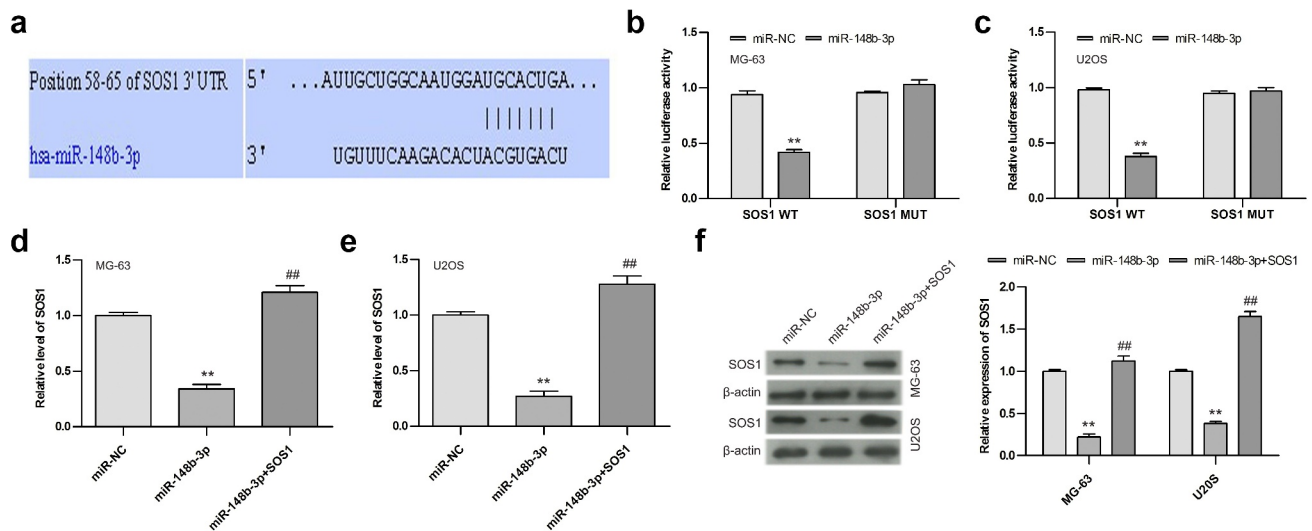


Figure 6. miR-148b-3p directly binds to SOS1. (a) The possible target site of miR-148b-3p on SOS1-wt were predicted by Targetscan online. (b) Relative luciferase activities in MG-63 cells was examined employing dual luciferase reporter gene. (c) Relative luciferase activities in U2OS cells was examined employing dual luciferase reporter gene. (d) The expression level of SOS1 in MG-63 cells was analyzed using qRT-PCR. (e) The expression level of SOS1 in U2OS cells was analyzed using qRT-PCR. (f) The expression of SOS1 in MG-63 and U2OS was analyzed by WB assay. **P < 0.01 versus miR-NC; ##P < 0.01 versus miR-148b-3p.

SOS1 over-expression reversed the anti-tumor effect of miR-148b-3p on OS cells

In order to in depth evaluate the inhibitory function of miR-148b-3p, we transfected SOS1 into OS cells pretreated with miR-148b-3p and named it as miR-148b-3p + SOS1 group. We found that miR-148b-3p mimic inhibited the clone formation of MG-63 and U2OS cells (Figure 7a), and overexpression of SOS1 significantly offset the inhibiting effect of miR-148b-3p mimic on OS cells proliferation. Furthermore, miR-148b-3p mimic significantly reduced the percentage of wound closure (Figure 7b) and the number of migratory cells (Figure 7c), but the difference between miR-NC and miR-148b-3p+SOS1 groups were not obvious. The result in Figure 7d displayed that miR-148b-3p mimic group had a higher apoptotic rate than miR-NC and miR-148b-3p + SOS1 group, and the difference between miR-NC and miR-148b-3p + SOS1 groups were not obvious. Together, miR-148b-3p suppressed the proliferation, migration and invasion, and stimulated apoptosis of OS cells, and over-expression of SOS1 could counteract these changes.

SOS1 silencing antagonized the effect of miR-148b-3p on the biological behavior of OS cells

Next, We transfected si-SOS1 into OS cells pretreated with miR-148b-3p inhibitor and named it as inhibitor + si-SOS1 group. We found that miR-148b-3p inhibitor promoted the clone formation of MG-63 and U2OS cells (Figure 8a). si-SOS1 significantly offset the promotion of miR-148b-3p inhibitor on OS cells proliferation. Furthermore, miR-148b-3p inhibitor significantly increased the percentage of wound closure (Figure 8b) and the number of migratory cells (Figure 8c), and the difference between the NC-inhibitor and inhibitor + si-SOS1 groups were not obvious. Flow cytometry displayed that miR-148b-3p inhibitor group had a lower apoptotic rate than NC-inhibitor and inhibitor + si-SOS1 group (Figure 8d). Together, miR-148b-3p inhibitor stimulated the proliferation, migration and invasion, and inhibited apoptosis of OS cells, and si-SOS1 could counteract these changes.

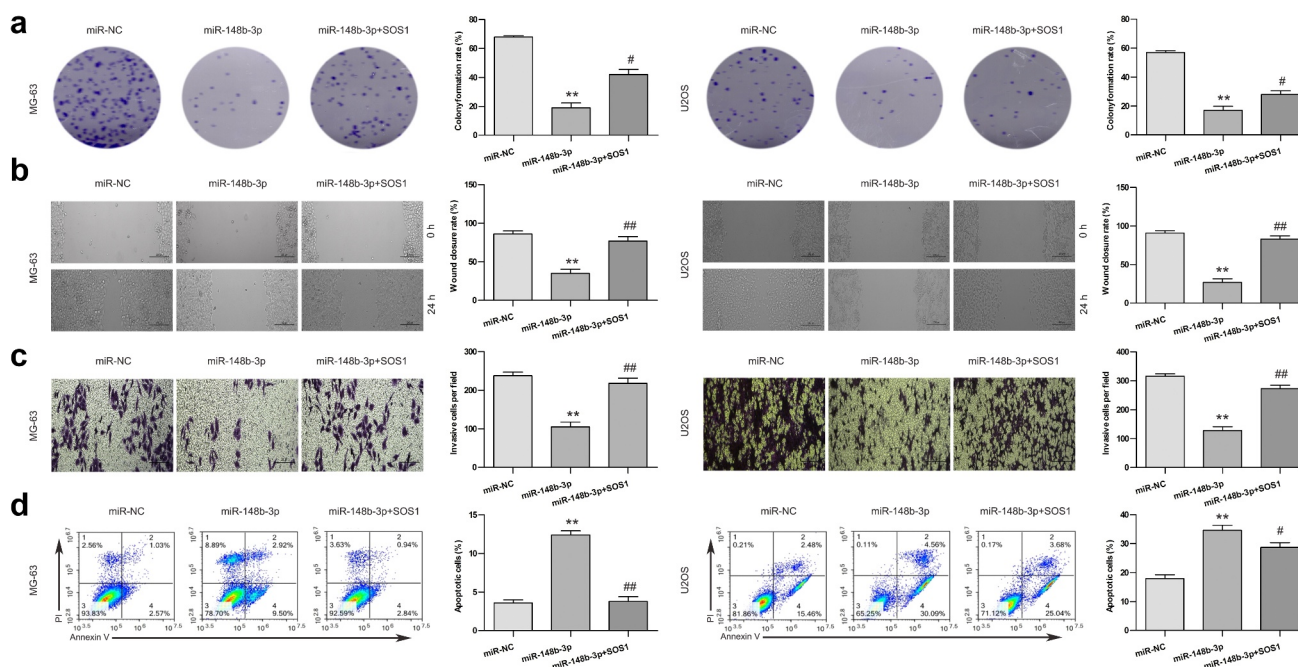


Figure 7. SOS1 overexpression reversed the anti-tumor effect of miR-148b-3p. (a) The colony number of OS cell were counted by colony formation assay. (b) The migratory ability of OS cells were measured using wound healing test, scale bars = 200 μ m. (c) The invasive ability of OS cells were using transwell invasion assay, scale bars = 200 μ m. (d) The apoptotic rate of OS cells was checked using flow cytometry. **P < 0.01 versus miR-NC; #P < 0.05, ##P < 0.01 versus miR-148b-3p.

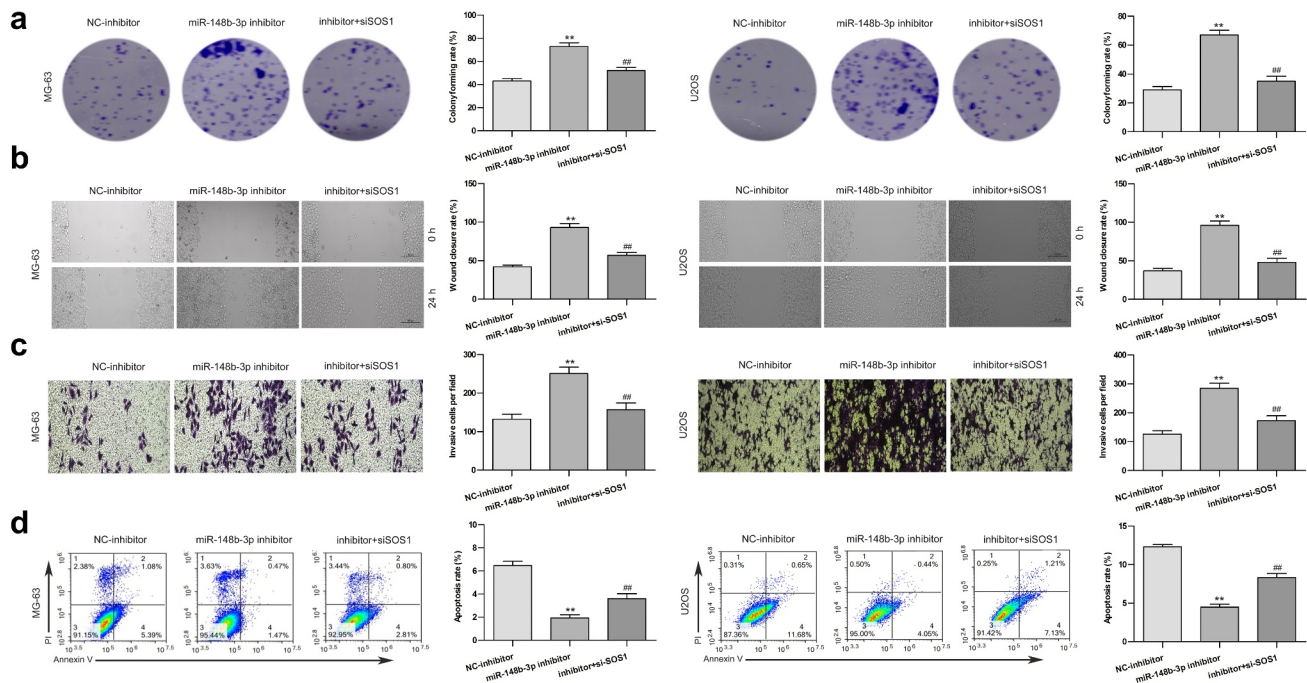


Figure 8. SOS1 silencing reversed the anti-tumor effect of miR-148b-3p. (a) The colony number of OS cell were counted by colony formation assay. (b) The migratory ability of OS cells were measured using wound healing test, scale bars = 200 μ m. (c) The invasive ability of OS cells were using transwell invasion assay, scale bars = 200 μ m. (d) The apoptotic rate of OS cells was checked using flow cytometry. ** $P < 0.01$ versus NC-inhibitor; # $P < 0.05$, ## $P < 0.01$ versus miR-148b-3p inhibitor.

miR-148b-3p over-expression inhibits xenograft tumor growth *in vivo*

In vivo, we established a tumor-bearing mouse model (Figure 9a) to study the role of miR-148b-3p on OS tumorigenesis, and about 5×10^6 MG-63 cells transfected with agomir-NC/-miR-148b-3p were injected into BALB/c nude mice ($n = 5$). Compared with agomir-NC, the tumor volume (Figure 9b) and weight (Figure 9c) was evidently reduced, and miR-148b-3p was significantly highly expressed in agomir group (Figure 9d). qRT-PCR (Figure 9d) and WB (Figure 9e) analysis demonstrated that over-expressed miR-148b-3p attenuated SOS1 expression. In addition, IHC analysis showed decreased Ki67 and MMP9, and increased cleaved-caspase-3 in the agomir group (Figure 9f). These findings further confirmed that miR-148b-3p inhibited OS growth via down-regulating SOS1 *in vivo*.

Discussion

In the present study, we observed that miR-148b-3p was obviously down-regulated in OS tissue specimens,

consistent with previous reports [14]. In addition, the level of miR-148b-3p was lower in OS cells compared with normal osteoblasts hFOB1.19 cell. miR-148b-3p mimic suppressed the OS cell growth, migration and invasion, and induced apoptosis. Conversely, miR-148b-3p-inhibitor promoted the cell growth, migration and invasion, and restrained apoptosis of OS cells. Significantly, miR-148b-3p inhibited the tumor growth of nude xenograft tumor *in vivo*. Our data strongly demonstrated that miR-148b-3p played a tumor suppressor role in OS progression. This report is the first evidence to indicate the regulatory role of miR-148b-3p on the malignant phenotypes of OS cells.

miRNAs are a class of endogenous and highly conserved small strand RNA [22], which are associated with the tumorigenesis of various cancers [9,23]. Some certain miRNAs show significant specific abnormal expression in cancers [10,24]. As an oncogene or tumor suppressor, miRNA has proven potential as a diagnostic marker for cancer [25]. Likewise, the researchers have found that dysfunctional miRNAs mediated cell proliferation, migration, invasion, and apoptosis in OS progression. For example, miR-335

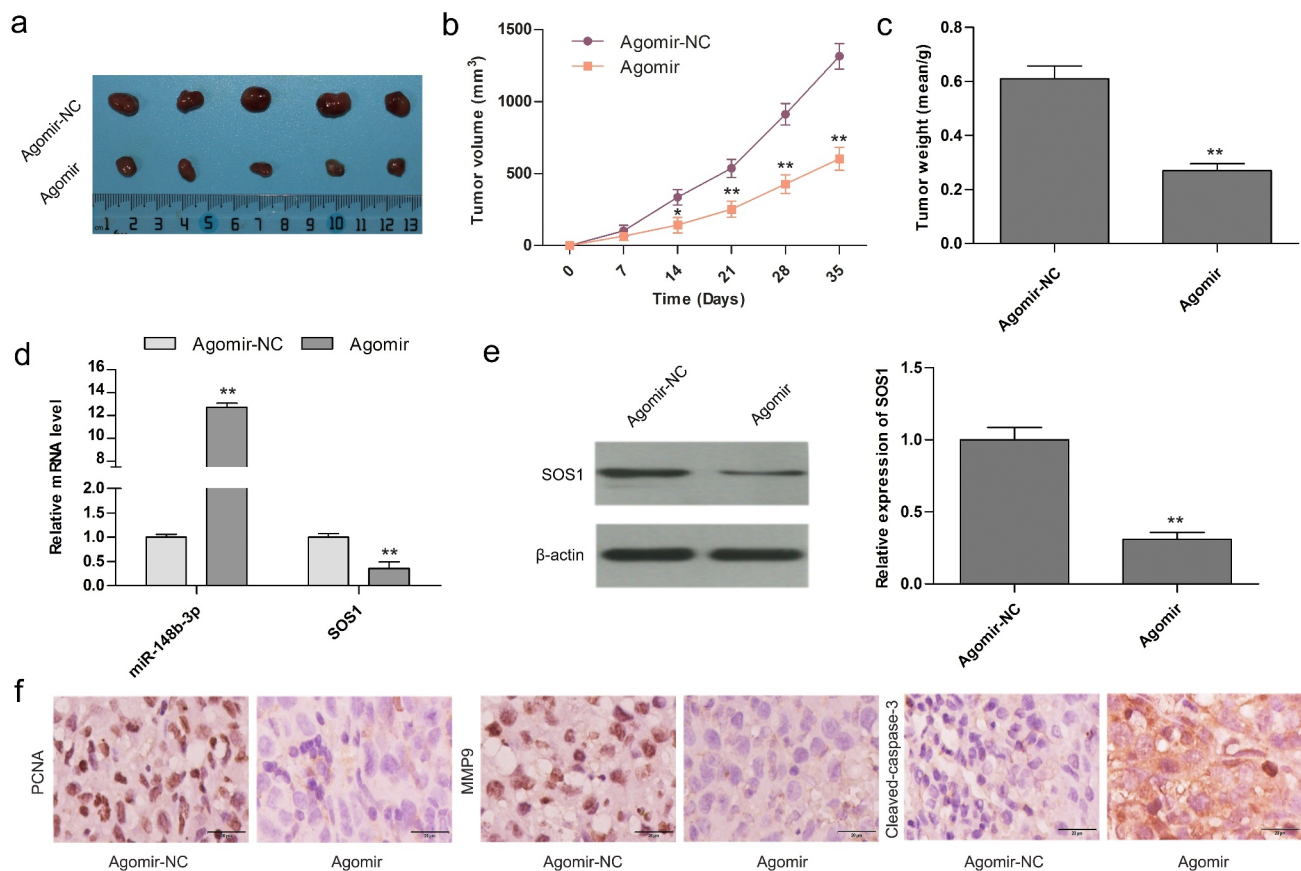


Figure 9. Over-expression of miR-148b-3p controlled tumor growth in mouse models. (a) Tumor photos from tumor-bearing mice with Agomir-NC and Agomir. Quantification of tumor size (b) and weight (c) post 35 days. (d) The mRNA levels of miR-148b-3p and SOS1 were measured using qRT-PCR. (e) The expression of SOS1 was analyzed by WB assay. (f) The expression of PCNA, MMP9 and cleaved-caspase-3 were analyzed by IHC staining. * $P < 0.05$, ** $P < 0.01$ versus Aogmir-NC.

was down-regulated and suppressed the OS cell growth and metastasis [26]. The expression of miR-16-5p was down-regulated in OS, and over-expression of miR-16-5p interfered with the metastasis of OS cells [27]. miR-143 was down-regulated and promoted apoptosis and suppressed tumorigenesis in OS [28].

It has been reported that miR-148b-3p is abnormal in different cancers, and miR-148b-3p is considered to be a tumor suppressor [11–13]. For instance, the mRNA levels of miR-148b-3p in glioma cells were obvious lower than in human astrocytes [29]. miR-148-3p was down-regulated in OS tissues and affected poor clinical prognosis [14]. However, the molecular mechanisms by which miR-148-3p regulates the malignant progression of OS cells remain unclear. Our research provided convincing results that miR-148-3p was poorly expressed both in OS tissues and cells, over-expression of miR-148-3p apparently inhibited the malignant biological behavior, and

inhibition of miR-148-3p clearly promoted the malignant biological behavior of OS cells, which supported the view that miR-148-3p suppresses tumor progression.

miRNAs are widely present in eukaryotes and play an important functional role by targeting downstream genes. In this study, TargetsCan tool calculated miR-148-3p bind to 3' -UTRs of SOS1, which was supported by the results of dual-luciferase reporter gene. Extensive evidence revealed that SOS1 was over-expressed in a variety of cancers [30,31]. Furthermore, SOS1 expression was elevated in epithelial ovarian cancer with high metastatic potential [31]. SOS1 knockdown suppressed EMT biological process in ovarian cancer [32]. Here, we observed that SOS1 was significantly overexpressed in OS tissues and cells, which was negatively correlated with miR-148-3p expression. Ulteriorly, the SOS1 over-expression or silencing rescued the anti-tumor

effect of miR-148-3p mimic or inhibitor on OS progression. Our research provided strong evidence for targeted regulation of miR-148-3p and SOS1 in OS.

Conclusions

Overall, we discovered that miR-148b-3p was evidently down-regulated both in OS tissues and cells, and miR-148b-3p mimic weakened the proliferation, migration and invasion, and induced apoptosis of OS cells. Importantly, our study also demonstrated that miR-148b-3p directly bound to SOS1, and miR-148b-3p regulated the malignant progression of OS cells by down-regulating SOS1. Therefore, miR-148b-3p acts a suppressor role in OS, and the present research provided a novel perspective into the treatment of OS patients. It should be noted that the malignant process of OS is very complex, and more researches are needed to further enrich the database.

Disclosure statement

No potential conflict of interest was reported by the author(s).

Funding

This work was supported by the Inner Mongolia Autonomous Region (IMAR) Natural Science Foundation under Grant [2016MS08119]; Inner Mongolia Autonomous Region (IMAR) Natural Science Foundation under Grant [2019MS08043].

ORCID

Xiaoyan Zhang  <http://orcid.org/0000-0002-8977-3477>

References

- [1] Morrow JJ, Khanna C. Osteosarcoma genetics and epigenetics: emerging biology and candidate therapies. *Crit Rev Oncog*. 2015;20:173–197.
- [2] Belayneh R, Fourman MS, Bhogal S, et al. Update on osteosarcoma. *Curr Oncol Rep*. 2021;23:71.
- [3] Chen Y, Cao J, Zhang N, et al. Advances in differentiation therapy for osteosarcoma. *Drug Discov Today*. 2020;25:497–504.
- [4] Tang H, Tang Z, Jiang Y, et al. Pathological and therapeutic aspects of matrix metalloproteinases: implications in osteosarcoma. *Asia Pac J Clin Oncol*. 2019;15:218–224.
- [5] Luetke A, Meyers PA, Lewis I, et al. Osteosarcoma treatment—where do we stand? A state of the art review. *Cancer Treat Rev*. 2014;40:523–532.
- [6] Harrison DJ, Geller DS, Gill JD, et al. Current and future therapeutic approaches for osteosarcoma. *Expert Rev Anticancer Ther*. 2018;18:39–50.
- [7] Tsuda Y, Tsoi K, Parry MC, et al. Impact of chemotherapy-induced necrosis on event-free and overall survival after preoperative MAP chemotherapy in patients with primary high-grade localized osteosarcoma. *Bone Joint J*. 2020;102-B:795–803.
- [8] Bartel DP. MicroRNAs: target recognition and regulatory functions. *Cell*. 2009;136(2):215–233.
- [9] Rupaimoole R, Slack FJ. MicroRNA therapeutics: towards a new era for the management of cancer and other diseases. *Nat Rev Drug Discov*. 2017;16(3):203–222.
- [10] Lu J, Getz G, Miska EA, et al. MicroRNA expression profiles classify human cancers. *Nature*. 2005;435(7043):834–838.
- [11] Zhang H, Ye Q, Du Z, et al. MiR-148b-3p inhibits renal carcinoma cell growth and pro-angiogenic phenotype of endothelial cell potentially by modulating FGF2. *Biomed Pharmacother*. 2018;107:359–367.
- [12] Li X, Jiang M, Chen D, et al. miR-148b-3p inhibits gastric cancer metastasis by inhibiting the Dock6/Rac1/Cdc42 axis. *J Exp Clin Cancer Res*. 2018;37(1):71.
- [13] Wang Y, Li J, Kuang D, et al. miR-148b-3p functions as a tumor suppressor in GISTs by directly targeting KIT. *Cell Commun Signal*. 2018;16(1):16–32.
- [14] Lin W, Wang L, Yang S, et al. Analysis of miR-148b expression differences in stage-I and II parosteal osteosarcoma. *Oncol Lett*. 2018;16(1):998–1002.
- [15] Zhao R, Song J, Jin Y, et al. Long noncoding RNA HOXC-AS3 enhances the progression of cervical cancer via activating ErbB signaling pathway. *J Mol Histol*. 2021;52(5):991–1006.
- [16] Baltanás FC, Zarich N, Rojas-Cabañeros JM, et al. SOS GEFs in health and disease. *Biochim Biophys Acta Rev Cancer*. 2020;1874(2):188445.
- [17] Chen H, Wu X, Pan ZK, et al. Integrity of SOS1/EPS8/AB11 tri-complex determines ovarian cancer metastasis. *Cancer Res*. 2010;70:9979–9990.
- [18] Huntzinger E, Izaurralde E. Gene silencing by microRNAs: contributions of translational repression and mRNA decay. *Nat Rev Genet*. 2011;12:99–110.
- [19] Kim DW, Kim KB, Kim JY, et al. Negative regulation of neuronal cell differentiation by INHAT subunit SET/TAF-I β . *Biochem Biophys Res Commun*. 2010;400:419–425.
- [20] Wu Q, Xu C, Zeng X, et al. Tumor suppressor role of sFRP-4 in hepatocellular carcinoma via the Wnt/ β -catenin signaling pathway. *Mol Med Rep*. 2021;23:5.
- [21] Xie Y, Sun W, Deng Z, et al. MiR-302b suppresses osteosarcoma cell migration and invasion by targeting Runx2. *Sci Rep*. 2017;7(1):13388.

- [22] Chen X, Ba Y, Ma L, et al. Characterization of microRNAs in serum: a novel class of biomarkers for diagnosis of cancer and other diseases. *Cell Res.* **2008**;18(10):997–1006.
- [23] Hu Y, Dingerdissen H, Gupta S, et al. MicroRNA: a signature for cancer progression. *Biomed Pharmacother.* **2021**;138:111528.
- [24] Hu Y, Dingerdissen H, Gupta S, et al. Identification of key differentially expressed MicroRNAs in cancer patients through pan-cancer analysis. *Comput Biol Med.* **2018**;103:183–197.
- [25] Stavast CJ, Erkeland SJ. The non-canonical aspects of MicroRNAs: many roads to gene regulation. *Cells.* **2019**;8(11):1456.
- [26] Xie Y, Deng H, Wei R, et al. Overexpression of miR-335 inhibits the migration and invasion of osteosarcoma by targeting SNIP1. *Int J Biol Macromol.* **2019**;133:137–147.
- [27] Gu Z, Li Z, Xu R, et al. miR-16-5p suppresses progression and invasion of osteosarcoma via targeting at Smad3. *Front Pharmacol.* **2020**;11:1324.
- [28] Zhang H, Cai X, Wang Y, et al. MicroRNA-143, down-regulated in osteosarcoma, promotes apoptosis and suppresses tumorigenicity by targeting Bcl-2. *Oncol Rep.* **2010**;24:1363–1369.
- [29] Wang G, Li Z, Tian N, et al. miR-148b-3p inhibits malignant biological behaviors of human glioma cells induced by high HOTAIR expression. *Oncol Lett.* **2016**;12:879–886.
- [30] Lv Z, Yang L. miR-124 inhibits the growth of glioblastoma through the downregulation of SOS1. *Mol Med Rep.* **2013**;8(2):345–349.
- [31] Cheng M, Ye X, Dai J, et al. SOS1 promotes epithelial-mesenchymal transition of Epithelial Ovarian Cancer (EOC) cells through AKT independent NF- κ B signaling pathway. *Transl Oncol.* **2021**;14(9):101160.
- [32] Fang D, Chen H, Zhu JY, et al. Epithelial-mesenchymal transition of ovarian cancer cells is sustained by Rac1 through simultaneous activation of MEK1/2 and Src signaling pathways. *Oncogene.* **2017**;36(11):1546–1558.